

Stochastic analysis of effective rate constant for heterogeneous reactions

P. C. Lichtner, D. M. Tartakovsky

Abstract. A probability density function (pdf) formulation is applied to a heterogeneous chemical reaction involving an aqueous solution reacting with a solid phase in a batch. This system is described by a stochastic differential equation with multiplicative noise. Both linear and nonlinear kinetic rate laws are considered. An effective rate constant for the mean field approximation describing the change in mean concentration with time is derived. The effective rate constant decreases with increasing time eventually approaching zero as the system approaches equilibrium. This behavior suggests that a possible explanation for the observed discrepancy between laboratory measured rate constants on uniform grain sizes and field measurements may in part be caused by the heterogeneous distribution of grain sizes in natural systems.

Keywords: Reactive transport, Random, Probability density function

1

Introduction

Within the geochemical community a controversy arose over the use of laboratory determined kinetic rate constants to describe field weathering rates. Early studies found a discrepancy of several orders of magnitude between field and laboratory estimated rate constants (Paces, 1983; Vebl, 1986). Since these studies, Lichtner (1993) and Sverdrup and Warfvinge (1995) and others, pointed out a number of flaws in the early rate estimates of field weathering rates involving the failure to properly account for various factors in the chemical rate laws that were used. An aspect that has not been thoroughly investigated, however, is the role of heterogeneous distributions of mineral grain sizes on weathering rates. The purpose of this study is to consider the implications of a heterogeneous grain size distribution on the governing equations for reactive

P. C. Lichtner, D. M. Tartakovsky (✉)
Los Alamos National Laboratory, Los Alamos, NM 87545, USA

This work was supported in part by the US Department of Energy under the DOE/BES Program in the Applied Mathematical Sciences, Contract KC-07-01-01, and the Environmental Management Science Program, Office of Biological and Environmental Research. This work made use of shared facilities supported by SAHRA (Sustainability of Semi-Arid Hydrology and Riparian Areas) under the STC Program of the National Science Foundation under agreement EAR-9876800. Los Alamos National Laboratory is operated by the University of California for the US Department of Energy under contact W-7405-ENG-36.

transport. Time and scale dependent effective retardation factors have been reported in the literature (e.g. Rajaram, 1997), and there is no reason not to expect similar behavior for effective kinetic rate constants.

It is not at all obvious that conventional continuum-based reactive transport formulations can provide an adequate description of reactions involving heterogeneous mineral grain size distributions. These models are developed from a phenomenological formulation involving macroscale properties obtained by averaging over a control volume. Kinetic reaction rates for mineral precipitation/dissolution reactions are related to an average mineral grain size associated with each control volume. Obviously, the conventional continuum approach does not account for effects that may be caused by a distribution of different grain sizes, and resulting surface areas, within a control volume.

Unfortunately our ability to upscale reactive transport processes involving complex multicomponent systems in a rigorous fashion is still in an early developmental stage. This is due to several reasons, but perhaps the most important is the inherent nonlinearity in the governing equations. This nonlinearity arises through kinetic rate laws describing precipitation/dissolution of solids and kinetic sorption/desorption rates, as well as through incorporation of local equilibrium relations derived from the law of mass action for homogeneous and heterogeneous reactions. Characteristic of the constitutive relations representing these processes is the appearance of products of species activities raised to integral and nonintegral powers (Lichtner, 1996). These nonlinear terms render conventional upscaling techniques such as volume averaging (Kechagia et al., 2002; Wood et al., 2000) and stochastic methods (Dagan and Indelman, 1999; Espinoza and Valocchi, 1997; Miralles-Wilhelm and Gelhar, 2000; Reichle et al., 1998) difficult to implement. Generally these approaches require expanding the nonlinear terms about the local mean concentration of the system retaining only linear terms. As a consequence such approaches only apply to small deviations from the mean – an approach that is inadequate for most natural geochemical systems.

In general, one would expect a heterogeneous distribution of minerals to result in time and space dependent effective rate parameters caused by progressively increased statistical sampling of the heterogeneous distribution over time. This stochastic induced space-time dependence of the effective parameters implies that these parameters cannot be treated as constants as is often done in conventional reactive transport models. Heterogeneous porous media composed of an aggregate of mineral grains involve a distribution of grain sizes, typically over a wide range of values. For such media the usual continuum approach based on a mean surface area for each reacting mineral may not be adequate. The discussion which follows is restricted to a simple batch system involving precipitation and dissolution of a single component phase with linear and nonlinear kinetics. This system corresponds to reaction of quartz, for example, involving a known initial distribution of grain sizes. The change in concentration is described by a stochastic differential equation with multiplicative noise. Such an equation has been considered in the past by a number of authors including Kubo (1962), Risken (1989), and van Kampen (1992).

2

Problem formulation

Consider a heterogeneous reaction taking place in a closed container of the form

$$\alpha \mathcal{A} \rightleftharpoons \mathcal{A}_{(s)} \quad , \quad (1)$$

between a dissolved species \mathcal{A} with concentration c and a solid $\mathcal{A}_{(s)}$ with stoichiometric coefficient α . The aqueous solution and solid are assumed to be well mixed, eliminating possible concentration gradients within the container. The solid phase consists of a mixture of different grain sizes resulting in a probability distribution p_k for the effective rate constant k . The latter is defined as $k = k_0 A C_{\text{eq}}^{1-\alpha}$, a product of the specific solid surface area A , the laboratory measured rate constant k_0 for reaction Eq. (1), and the power of the equilibrium concentration C_{eq} associated with reaction Eq. (1). The change in aqueous concentration is described by the stochastic differential equation

$$\frac{dc}{dt} = -\alpha k (c^\alpha - C_{\text{eq}}^\alpha) . \quad (2)$$

The equilibrium concentration C_{eq} is assumed to be deterministic as determined from thermodynamic considerations. Equation. (2) is subject to the initial condition

$$c(0) = C_0 , \quad (3)$$

where the initial concentration C_0 is assumed to be deterministic for simplicity. The initial concentration may be greater or less than the equilibrium concentration resulting in precipitation or dissolution of the solid, respectively. The change in solid concentration is considered to be negligible. The notation used in the following reserves upper case names for deterministic variables and constants and lower case for random variables.

Equation (2) applies to a length scale that is much larger than the separation between solid grains, but smaller than the dimensions of the container. Thus Eq. (2) refers to a macroscale continuum formulation but involving a random variable for the effective rate constant. This equation breaks down when the reaction rate becomes large enough to produce gradients on the scale of the separation between solid grains. In such cases it is necessary to explicitly account for diffusion-controlled reaction at the surface of the solid grains. In addition, k is assumed to be independent of time. For the case of dissolution, as reaction proceeds the surface may in fact increase with time due to the formation of etch pits on the mineral surface. As individual grains completely dissolve the associated surface area would tend to zero. For the system considered here, it is assumed that equilibrium is reached before appreciable changes in grain surface can occur. For the case of precipitation it is assumed that the precipitating solid nucleates on the existing mineral surface although this need not necessarily be the case in general. Surface armoring effects, not considered here, could also result in a time-dependent surface area. Although simplistic, Eq. (2) has the distinct advantage of possessing an analytical solution, thus enabling one to discern properties of upscaled effective rate constant in detail. The case of time-dependent k is left for future investigation.

The single point pdf p_k , representing the stochastic rate constant, $k(\mathbf{x})$ is usually obtained indirectly from the grain size distribution p_l . The two distributions are related through the assumption made for the relation between surface and grain size. For example, for cubical grains with side l , the specific surface area a is given by

$$a = \frac{6\lambda\phi_s}{l} , \quad (4)$$

where ϕ_s is the fraction of volume occupied by the solid, and λ represents a roughness factor. It follows that with $k = k_0 a$,

$$p_k(k) = p_l(l) \frac{dl}{dk} = \frac{6\lambda\phi_s k_0}{k^2} p_l\left(\frac{6\lambda\phi_s k_0}{k}\right) . \quad (5a)$$

Other assumptions, of course, are also possible such as spherical grains. The pdf for the grain size distribution is assumed to follow a log normal distribution (Clausnitzer and Hopmans, 1999; Tuli et al., 2001).

$$p_l(l) = \frac{1}{l\sigma_l^2\sqrt{2\pi}} e^{-(\ln l - \mu_l)^2 / (2\sigma_l^2)} . \quad (5b)$$

Figure 1 shows the distribution p_k in Eq. (5), for $\mu_l = 1$ and $\sigma_l^2 = 1$. Both k and p_k are normalized with $6\lambda\phi_s k_0$. Multi-point correlation structure is required to complete the description of a random field $k(\mathbf{x})$. However, since flow is absent in the batch system described by Eq. (2), the upscaled effective reaction rate is independent of a correlation function and is specified fully by the single-point pdf p_k .

In the presence of flow, Eq. (2) provides a Lagrangian description of reactive transport. In this case, to make the analyses below applicable, it is necessary to assume that the correlation length, λ_k , of the random field $k(\mathbf{x})$ is much larger than the characteristic length of the batch system. This corresponds to setting $\lambda_k = \infty$, i.e., treating the effective reaction rate k as a random constant. Each realization of the column consists of a uniform grain size (effective rate constant) sampled from the grain size (rate constant) distribution.

Equation (2) represents a stochastic first order ordinary differential equation with multiplicative noise. The concentration $c(t)$ obtained as the solution of Eq. (2) is a random field determined implicitly as a formal solution of the equation

$$\int_{c_0}^{c(t)} \frac{dc'}{c'^\alpha - C_{eq}^\alpha} = -\alpha kt . \quad (6)$$

The integral can be expressed in terms of the hypergeometric function ${}_2F_1(a, b, c, x)$ to give

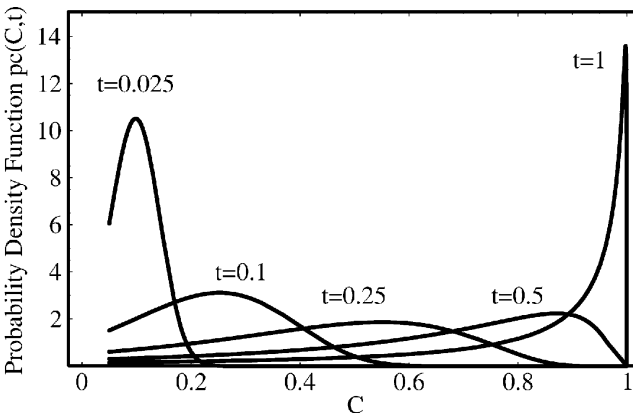


Fig. 1. Probability density function for the effective rate

$$\left(\frac{c}{C_{\text{eq}}^\alpha}\right) {}_2F_1\left[\frac{1}{\alpha}, 1, 1 + \frac{1}{\alpha}, \left(\frac{c}{C_{\text{eq}}}\right)^\alpha\right] - \left(\frac{C_0}{C_{\text{eq}}^\alpha}\right) {}_2F_1\left[\frac{1}{\alpha}, 1, 1 + \frac{1}{\alpha}, \left(\frac{C_0}{C_{\text{eq}}}\right)^\alpha\right] = \alpha kt . \quad (7)$$

From this result explicit solutions are obtained for the linear reaction case ($\alpha = 1$),

$$c(t) = (C_0 - C_{\text{eq}})e^{-kt} + C_{\text{eq}} \quad (8)$$

and for the nonlinear reaction case ($\alpha = 2$),

$$\frac{c(t)}{C_{\text{eq}}} = 2 \left(1 - \frac{C_0 - C_{\text{eq}}}{C_0 + C_{\text{eq}}} e^{-2kt}\right)^{-1} - 1 . \quad (9)$$

For sufficiently long times, $kt \gg 1$, in either case the concentration approaches the deterministic equilibrium concentration C_{eq} .

3

PDF solution

Formulation of the partial differential equation for the pdf equivalent to the stochastic differential equation Eq. (2) is based on the observation that the ensemble mean of the function

$$\Pi(c, C; t) \equiv \delta(c(t) - C) \quad (10)$$

where $\delta(\cdot)$ denotes the Dirac delta function, is the one-point pdf for concentration,

$$p_c(C, t) = \langle \Pi(c, C; t) \rangle . \quad (11)$$

In these expressions c denotes a random variable, whereas C is a real non-negative number. The partial differential equation satisfied by p_c is derived by noting that

$$\frac{\partial \Pi}{\partial t} = \frac{\partial \Pi}{\partial c} \frac{dc}{dt} = - \frac{\partial \Pi}{\partial C} \frac{dC}{dt} = \alpha k (c^\alpha - C_{\text{eq}}^\alpha) \frac{\partial \Pi}{\partial C} , \quad (12a)$$

taking into account Eq. (2), and

$$(c^\alpha - C_{\text{eq}}^\alpha) \frac{\partial \Pi}{\partial C} = \frac{\partial}{\partial C} [(c^\alpha - C_{\text{eq}}^\alpha) \Pi] = \frac{\partial}{\partial C} [(c^\alpha - C_{\text{eq}}^\alpha) \delta(c - C)] = \frac{\partial}{\partial C} [(C^\alpha - C_{\text{eq}}^\alpha) \Pi] . \quad (12b)$$

Hence the following equation for Π is obtained

$$\frac{\partial \Pi}{\partial t} = -\alpha k \frac{\partial}{\partial C} [(C^\alpha - C_{\text{eq}}^\alpha) \Pi] . \quad (13)$$

Taking the ensemble mean yields the equation

$$\frac{\partial p_c}{\partial t} = -\alpha \frac{\partial}{\partial C} [(C^\alpha - C_{\text{eq}}^\alpha) \langle k\Pi \rangle] , \quad (14)$$

involving p_c . Using the Reynolds decomposition, $k = \langle k \rangle + k'$ and $\Pi = p_c + \Pi'$ with $\langle k' \rangle = \langle \Pi' \rangle = 0$, gives

$$\frac{\partial p_c}{\partial t} + \alpha \langle k \rangle \frac{\partial}{\partial C} [(C^\alpha - C_{\text{eq}}^\alpha) p_c] = -\alpha \frac{\partial}{\partial C} [(C^\alpha - C_{\text{eq}}^\alpha) \langle k' \Pi' \rangle] . \quad (15)$$

In order to solve the pdf equation for p_c it is necessary to know the correlation $\langle k\Pi \rangle$ in terms of the pdf p_c .

An exact solution to the pdf equation for p_c , Eq. (14) or Eq. (15), can be obtained through the coordinate transformation from C to $K_x(C, t)$ where K_x is obtained from the relation

$$K_x(C, t) = -\frac{1}{\alpha t} \int_{C_0}^C \frac{dC'}{C'^\alpha - C_{\text{eq}}^\alpha} . \quad (16)$$

Thus it is possible to relate p_c and p_k through the transformation

$$p_c(C, t) dC = p_k(K_x) dK_x , \quad (17)$$

or

$$p_c(C, t) = p_k(K_x) \left| \frac{\partial K_x}{\partial C} \right| = \frac{p_k[K_x(C, t)]}{\alpha t |C^\alpha - C_{\text{eq}}^\alpha|} . \quad (18)$$

where from Eq. (16)

$$\frac{\partial K_x}{\partial C} = -\frac{1}{\alpha t (C^\alpha - C_{\text{eq}}^\alpha)} . \quad (19)$$

An explicit form for K_x can be obtained from Eq. (7) in terms of the hypergeometric function.

An explicit expression for the correlation $\langle k\Pi \rangle$ is obtained by substituting the expression for p_c given by Eq. (18) into the partial differential equation, Eq. (14). This yields

$$\langle k\Pi \rangle = K_x(C, t) p_c(C, t) . \quad (20)$$

Similarly, higher order correlations have the explicit form

$$\langle (k')^n \Pi \rangle = (K_x(C, t) - \langle k \rangle)^n p_c(C, t) . \quad (21)$$

With this result the pdf for p_c is closed providing the partial differential equation

$$\frac{\partial p_c}{\partial t} = -\alpha \frac{\partial}{\partial C} \left[K_x(C, t) (C^\alpha - C_{\text{eq}}^\alpha) p_c(C, t) \right] . \quad (22)$$

It can be verified by direct substitution that the expression for p_c given in Eq. (18) satisfies Eq. (22).

In the limit $t \rightarrow \infty$, it follows that $p_c(C, t) \rightarrow \delta(C - C_{eq})$ as the reacting system approaches its final equilibrium state determined by the well-defined deterministic equilibrium concentration C_{eq} . Formally, this can be seen from the defining equations from the following argument. For any test function $f(C)$

$$\begin{aligned} \lim_{t \rightarrow \infty} \int f(C) p_c(C, t) dC &= \lim_{t \rightarrow \infty} \int f(C) p_k[K_x(C, t)] \left| \frac{dK_x}{dC} \right| dC, \\ &= \lim_{t \rightarrow \infty} \int f[C(t)] p_k(K_x) dK_x, \\ &= \int f(C_{eq}) p_k(K_x) dK_x = f(C_{eq}) , \end{aligned} \tag{23}$$

where $\lim_{t \rightarrow \infty} C(t) \rightarrow C_{eq}$ is used. Thus

$$\lim_{t \rightarrow \infty} p_c(C, t) \rightarrow \delta(C - C_{eq}) . \tag{24}$$

In addition, for $t = 0$, $p_c(C, 0) = \delta(C - C_0)$ as required by the initial condition with deterministic C_0 .

The time evolution of p_c corresponding to a gaussian distribution p_k is plotted in Fig. 2 as a function of C for different times. The initial concentration $C_0 = 0.05$ and the equilibrium concentration $C_{eq} = 1$. As can be seen from the figure, initially p_c corresponds to the delta function $\delta(C - C_0)$ and evolves with increasing time in the delta function $\delta(C - C_{eq})$.

4 Upscaled effective rate constant

The usual continuum formulation of the transport equation is based on an ensemble average of Eq. (2),

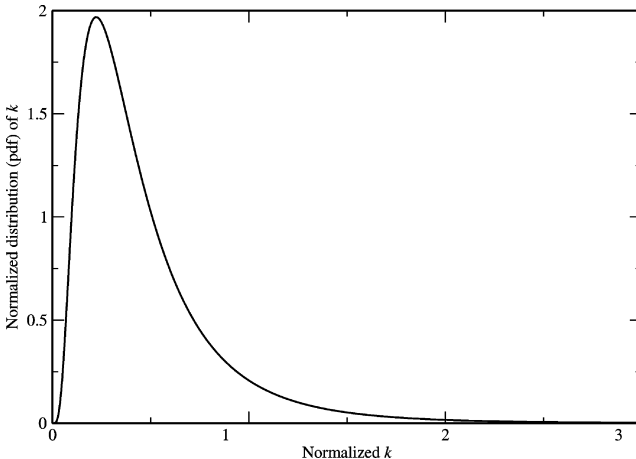


Fig. 2. Distribution $p_c(C, t)$ plotted as a function of time showing the time evolution from its initial distribution represented by the delta function $\delta(C - C_0)$ centered at $C_0 = 0.05$ to the final delta function $\delta(C - C_{eq})$ centered at $C_{eq} = 1$

$$\frac{d\langle c \rangle}{dt} = -\alpha k_{\text{eff}}(t) [\langle c \rangle^\alpha - C_{\text{eq}}^\alpha] . \quad (25)$$

To derive an expression for the upscaled effective rate, k_{eff} , we note that

$$\langle c(t) \rangle = \int C p_c(C, t) dC . \quad (26)$$

Taking the time derivative, while accounting for Eq. (22), yields

426

$$\begin{aligned} \frac{d\langle c \rangle}{dt} &= \int C \frac{\partial p_c}{\partial t} dC \\ &= \alpha \int C \frac{\partial}{\partial C} \left[K_\alpha(C, t) (C^\alpha - C_{\text{eq}}^\alpha) p_c \right] dC . \end{aligned} \quad (27)$$

Integrating by parts gives

$$\frac{d\langle c \rangle}{dt} = -\alpha \int K_\alpha(C, t) (C^\alpha - C_{\text{eq}}^\alpha) p_c dC . \quad (28)$$

Comparing Eqs. (25) and (28) defines the upscaled effective rate as

$$\begin{aligned} k_{\text{eff}}(t) &= \frac{1}{\langle c \rangle^\alpha - C_{\text{eq}}^\alpha} \int K_\alpha(C, t) (C^\alpha - C_{\text{eq}}^\alpha) p_c dC \\ &= \frac{1}{\langle c \rangle^\alpha - C_{\text{eq}}^\alpha} \int K_\alpha [C^\alpha(K_\alpha, t) - C_{\text{eq}}^\alpha] p_k(K_\alpha) dK_\alpha . \end{aligned} \quad (29)$$

From this result it is apparent that the upscaled effective rate varies in time. This finding is in line with earlier results that demonstrated a time dependence of the upscaled hydraulic conductivity for transient saturated flow (e.g., Tartakovsky and Neuman, 1998). It is easy to see that the effective rate has as initial value the mean value of k ,

$$k_{\text{eff}}(0) = \langle k \rangle . \quad (30)$$

Our expression for the upscaled effective reaction rate given in Eq. (29) allows for statistical inhomogeneity of the random field $k(\mathbf{x})$. It is important to point out however that it is independent of the correlation structure of $k(\mathbf{x})$.

We now proceed to explore the behavior of $k_{\text{eff}}(t)$ for two special cases: $\alpha = 1$ and $\alpha = 2$. In both cases, the random field $k(\mathbf{x})$ is assumed to be stationary, so that k_{eff} is independent of location \mathbf{x} .

For the linear rate law ($\alpha = 1$), substituting Eq. (8) into Eq. (26) one obtains for the mean concentration

$$\langle c \rangle = (C_0 - C_{\text{eq}}) \int e^{-Kt} p_k(K) dK + C_{\text{eq}} . \quad (31)$$

Thus for the linear case the expectation value of the concentration is directly proportional to the Laplace transform of the distribution p_k . The expression for k_{eff} in this case reduces to

$$k_{\text{eff}}(t) = \frac{\int K e^{-Kt} p_k(K) dK}{\int e^{-Kt} p_k(K) dK} = -\frac{d}{dt} \ln \langle e^{-kt} \rangle . \quad (32)$$

For $kt \ll 1$, $k_{\text{eff}}(t) \simeq \langle k \rangle$. Asymptotically, for $kt \gg 1$, $k_{\text{eff}} \rightarrow 0$.

For the nonlinear rate law with $\alpha = 2$, substituting Eq. (9) into Eq. (26) one obtains for the mean concentration

$$\frac{\langle c \rangle}{C_{\text{eq}}} = 2 \int \left(1 - \frac{C_0 - C_{\text{eq}}}{C_0 + C_{\text{eq}}} e^{-2Kt} \right)^{-1} p_k(K) dK - 1 . \quad (33)$$

Substituting Eqs. (9) and (33) and Eq. (4) into yields the corresponding expression for k_{eff} . Note that k_{eff} for the linear reaction rate law is a property of the porous medium only. This is not the case for the nonlinear reactions, where it also depends on the initial and equilibrium concentrations.

Figure 3 shows the upscaled effective reaction rate k_{eff} for $\alpha = 1$ and $\alpha = 2$ corresponding to the distribution p_k in Eq. (5). In these calculations, we used the parameters: $\mu_l = 1.0$, $\sigma_l = 1.0$ and $C_0 = 3C_{\text{eq}}$. With increasing time, the upscaled effective rate constant decreases approaching zero asymptotically, albeit slowly. This behavior is to be expected since as time increases the integrands in the numerator and denominator of Eq. (32) only contribute for $K \rightarrow 0$, which is equivalent to large grain size ($l \rightarrow \infty$). Thus the larger grain sizes become sampled statistically with greater weight. For the sharp distribution $p_k = \delta(K - K_0)$, it follows that $k_{\text{eff}} = K_0$ becomes constant.

This result also sheds light on the controversy over laboratory and field determined rate constants (Velbel, 1986). Field estimated mineral kinetic rate constants are found to differ sometimes by as much as several orders of magnitude from laboratory measured rate constants. While some of this discrepancy can be explained by the simplistic use of models (e.g. neglect of affinity factor in the rate expression, difficulty in estimating effective field surface area, etc.), the behavior of the effective rate constant derived in this work is consistent with such observations.

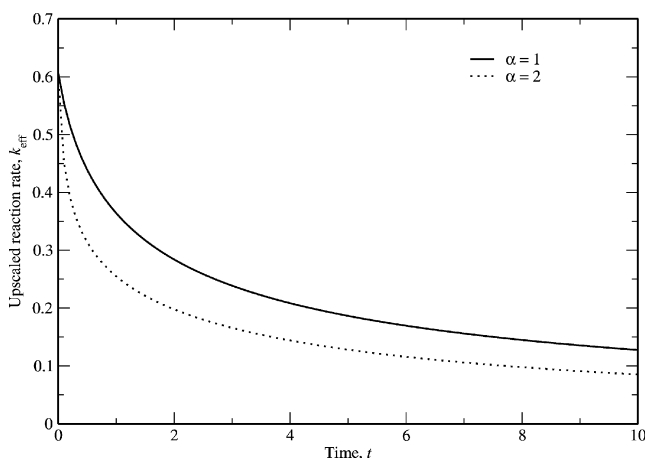


Fig. 3. The upscaled effective rate constant k_{eff} for the linear (solid line) and nonlinear with $\alpha = 2$ (dotted line) reaction laws

Conclusion

The effect of a stochastic rate parameter for reaction of a solute involving precipitation and dissolution with linear and nonlinear kinetic rate laws was investigated for a batch system. It was demonstrated that for a single component system containing a distribution of mineral grain sizes, the effective rate constant that appears in the differential equation for the change in mean concentration is a decreasing function of time. It can be expected that this same behavior will be present in more complex, multicomponent, systems involving fluid flow. The result is consistent with the observed discrepancy between field and laboratory based measurements of mineral kinetic rate constants.

References

- Clausnitzer V, Hopmans JW** (1999) Determination of phase-volume fractions from tomographic measurements in two-phase systems. *Adv. Water Resour.* 22(6): 577–584
- Dagan G, Indelman P** (1999) Reactive solute transport inflow between a recharging and a pumping well in a heterogeneous aquifer. *Water Resour. Res.* 35(12): 3639–3647
- Espinoza C, Valocchi AJ** (1997) Stochastic analysis of one-dimensional transport of kinetically adsorbing solutes in chemically heterogeneous aquifers. *Water Resour. Res.* 33(11): 2429–2445
- Kechagia P, Tsimpanogiannis IN, Yortsos YC, Lichtner PC** (2002) On the upscaling of reaction-transport processes in porous media with fast or finite kinetics. *Chem. Eng. Sci.* 57: 2565–2577
- Kubo R** (1962) A stochastic theory of line-shape and relaxation. In: *Fluctuation, Relaxation, and Resonance in Magnetic Systems*, ter Haar D (ed.), Oliver and Boyd, Edinburgh-London
- Lichtner PC** (1993) Scaling properties of time-space kinetic mass transport equations and the local equilibrium limit. *Am. J. Sci.* 293: 257–296
- Lichtner PC** (1996) Continuum formulation of multicomponent-multiphase reactive transport. In: *Reactive Transport in Porous Media*, Lichtner PC, Steefel CI, Oelkers EH (eds), *Reviews in Mineralogy*, vol. 34: pp. 1–81
- Miralles-Wilhelm F, Gelhar LW** (2000) Stochastic analysis of oxygen-limited biodegradation in heterogeneous aquifers with transient microbial dynamics. *J. Contam. Hydrol.* 42(1): 69–97
- Paces T** (1983) Rate constant of dissolution derived from the measurements of mass balances in catchments. *Geochim. Cosmochim. Acta* 47: 1855–1863
- Rajaram H** (1997) Time and scale dependent effective retardation factors in heterogeneous aquifers. *Adv. Wat. Res.* 20: 217–230
- Reichle R, Kinzelbach W, Kinzelbach H** (1998) Effective parameters in heterogeneous and homogeneous transport models with kinetic sorption. *Water Resour. Res.* 34(4): 583–594
- Risken H** (1989) *The Fokker-Planck Equation: Methods of Solution and Applications*, 2nd edn, Springer-Verlag, p. 472
- Sverdrup H, Warfvinge P** (1995) Estimating field weathering rates using laboratory kinetics. In: *Reviews in Mineralogy*, vol. 31, pp. 485–541
- Tartakovsky DM, Neuman SP** (1998) Transient effective hydraulic conductivities under slowly and rapidly varying mean gradients in bounded three-dimensional random media. *Water Resour. Res.* 34(1): 21–32
- Tuli A, Kosugi K, Hopmans JW** (2001) Simultaneous scaling of soil water retention and unsaturated hydraulic conductivity functions assuming lognormal pore-size distribution. *Adv. Water Resour.* 24: 677–688
- van Kampen NG** (1992) *Stochastic Processes in Physics and Chemistry*, Elsevier Science, p. 465
- Velbel M** (1986) The mathematical basis for determining rates of geochemical and geomorphic processes in small forested watersheds by mass balance. Examples and

implications. In: Coleman S, Dethier D (eds) Rates of Chemical Weathering of Rocks and Minerals, Academic Press, New York, pp. 439–451

Wood BD, Quintard M, Whitaker S (2000) Jump conditions at non-uniform boundaries: the catalytic surface. Chem. Eng. Sci. 55: 5231–5245